DERIVATION AND GENERAL PROPERTIES OF ARTIFICIAL LOSSLESS BALANCED COMPOSITE RIGHT/LEFT-HANDED TRANSMISSION LINES OF ARBITRARY ORDER

C. Camacho-Peñalosa and T. M. Martín-Guerrero

Departamento de Ingeniería de Comunicaciones
E.T.S. Ingeniería de Telecomunicación
Universidad de Málaga
E-29071 Málaga, Spain

J. Esteban and J. E. Page

Departamento de Electromagnetismo y Teoría de Circuitos
E.T.S. Ingeniería de Telecomunicación
Universidad Politécnica de Madrid
E-28071 Madrid, Spain

Abstract—A circuit theory-based approach for systematically deriving all possible lossless balanced composite right/left-handed transmission lines is described. To illustrate the usefulness of the proposed approach, novel artificial transmission line unit-cells with tri- and quad-band behaviour are proposed. It is shown that the number of right-handed or left-handed frequency bands exhibited by such transmission lines is determined by the order of its unit-cell. It is explained why artificial lossless balanced transmission lines exhibit a stop-band around each pole of their associated continuous transmission line that can not be closed up. Since this approach allows for the systematic derivation of such transmission line unit-cells of arbitrary order, multi-band components based on metamaterial transmission lines are envisaged.

Corresponding author: T. M. Martin-Guerrero (teresa@ic.uma.es, teresa@uma.es).

1. INTRODUCTION

Artificial transmission lines are lumped-element based circuits that can mimic the propagation characteristics of actual transmission lines. These circuits can emulate the propagation characteristics of TEM-based transmission systems filled with homogeneous, linear, and isotropic negative refraction index bulk media, despite the fact that such media have not yet been found or artificially realized. This is the physical foundation of the so-called 'metamaterial transmission line approach' used to study propagation phenomena in this kind of media and, more importantly, to develop and implement metamaterial-based engineering applications [1, 2].

The most basic lossless metamaterial transmission line is the so-called 'backward-wave' transmission line. Although it has been included in classical textbooks (see [3], for instance) for many years, it has not been approached as a 'left-handed' (LH) or metamaterial transmission line until very recently. This artificial transmission line exhibits backward-wave or LH behaviour, i.e., group and phase velocities are antiparallel [4], over an infinite range of frequencies. Since group velocity in lossless media (Foster's reactance theorem) is always positive, backward-wave or LH and conventional 'forward-wave' or 'right-handed' (RH) behaviours are associated, respectively, with negative and positive values of the imaginary part (β, phase constant) of the propagation constant.

From a practical point of view, the most interesting and useful lossless metamaterial transmission line proposed so far is the so-called 'composite right/left-handed' (CRLH) artificial transmission line [1, 2, 5]. It exhibits richer frequency behaviour and can be easily implemented in different microwave technologies. Many novel engineering applications involving metamaterials are based on this particular artificial transmission line.

More recently, new forms of metamaterial transmission lines have been proposed: the 'dual' [6], the 'extended' [7, 8], and the double-Lorentz [9] CRLH transmission lines. The 'dual' CRLH exhibits properties complementary to those presented by the 'conventional' CRLH transmission line, while keeping the dual-band frequency behaviour. On the contrary, the main feature of the 'extended' and the double-Lorentz CRLH-TLs is their potential as quad- and tri-band, respectively, components due to their more complex frequency behaviour.

In a general sense, CRLH transmission lines can be defined as artificial transmission lines which exhibit RH ($\beta > 0$) behaviour for certain frequency bands, and LH ($\beta < 0$) behaviour for other frequency

bands. The CRLH transmission line is said to be 'balanced' [1] when the distributed series impedance and the distributed shunt admittance have exactly the same critical frequencies (poles and zeros). The need for an exact match can be the main reason for the difficulties to achieve a perfect 'balance' in actual implementations. The aim of this work is to derive all possible lossless balanced CRLH transmission lines in a systematic way and using a circuit theory-based approach. As a result, already proposed artificial CRLH transmission lines are 'rediscovered' and classified in a natural manner, according to the order of their unit-cell, and many (infinite) new ones are obtained, although for simplicity, only some of them are described. An interesting conclusion is that artificial lossless balanced transmission lines exhibit stop-bands around each pole of their associated continuous transmission line that can not be closed up, which clearly limits the usable frequency range. Another interesting conclusion is that the number of RH and LH frequency bands in an artificial lossless balanced CRLH transmission line is governed by the order of its incremental unit-cell, which provides a design tool for metamaterial-based multi-band components.

2. THE IDEAL CONTINUOUS TRANSMISSION LINE

A continuous transmission line is fully characterized by its distributed (per-unit-length) series impedance $Z(s)$ and its distributed (per-unit-length) shunt admittance $Y(s)$ [3], where s is the complex frequency. The propagation constant $\gamma(s)$ and the characteristic impedance $Z_0(s)$ of this transmission line are given by

$$\gamma(s) = \sqrt{Z(s)Y(s)} \tag{1}$$

and

$$Z_0(s) = \sqrt{\frac{Z(s)}{Y(s)}} \tag{2}$$

respectively.

In the lossless case, $Z(\omega) = Z(s)|_{s=j\omega}$ and $Y(\omega) = Y(s)|_{s=j\omega}$ are purely imaginary, therefore $Z_0(\omega) = Z_0(s)|_{s=j\omega}$ is real and can be, under certain conditions, frequency independent. Under such circumstances, the continuous transmission line can easily be matched and propagates energy at all frequencies. This is the so-called 'balanced condition' or 'impedance matched condition' as defined in [1] and [2], respectively.

To achieve such a condition, namely $Z_0(s)|_{s=j\omega} = Z_0 \forall \omega$, $Z(\omega)$ and

$Y(\omega)$ must verify

$$\frac{Z(\omega)}{Y(\omega)} = Z_0^2 \tag{3}$$

that is,

$$\overline{Z}(\omega) = \frac{Z(\omega)}{Z_0} = \frac{Y(\omega)}{Y_0} = \overline{Y}(\omega) \tag{4}$$

and

$$\overline{Z}(\omega) = \overline{Y}(\omega) = \gamma(\omega) \tag{5}$$

with $Y_0 = Z_0^{-1}$, and $\gamma(\omega) = j\beta(\omega) = \gamma(s)|_{s=j\omega}$. This result means that, for obtaining a 'balanced' continuous transmission line, the normalized per-unit-length series impedance $\overline{Z}(\omega)$ and shunt admittance $\overline{Y}(\omega)$ must be identical, and therefore (and most importantly) the propagation constant is also identical to them. In practical terms, this means that the propagation characteristics of lossless balanced transmission lines are just those exhibited by the immittance function of a lossless one-port network. Therefore the propagation constant should be a real positive function with all poles and zeros on the $j\omega$ axis. This function can be, in general, expressed as [10]

$$\gamma(s) = \overline{Z}(s) = \overline{Y}(s) = \frac{K_0}{s} + \frac{2K_1 s}{s^2 + \omega_1^2} + \frac{2K_3 s}{s^2 + \omega_3^2} + \ldots + K_\infty s \tag{6}$$

Poles and zeros of real positive functions must alternate on the $j\omega$ axis, and there must be either a pole or a zero at $\omega = 0$ and at $\omega = \infty$ [10]. Any lossless balanced transmission line that satisfies (5) will exhibit an alternate left-handed/right-handed response, whether beginning with a left-handed band or with a right-handed one. As an example, a possible frequency response for a function like (6), and therefore, a particular dispersion diagram for a lossless balanced continuous transmission line, is shown in Fig. 1.

It is evident from Fig. 1 that the generic frequency dependence of the phase constant of any lossless balanced continuous transmission line exhibits frequency bands where $\beta > 0$ (RH behaviour) and others where $\beta < 0$ (LH behaviour). It is also clear that these bands, RH and LH regions, must alternate, and that the higher the order of the immittance function, the higher the total number of RH and LH regions in the propagation constant (increasing the complexity of the dispersion diagram). It can also be concluded that the first (lowest) frequency band may correspond to either RH or LH behaviour, depending on whether the distributed immittance function has a zero or a pole, respectively, at the origin. In particular, lossless balanced
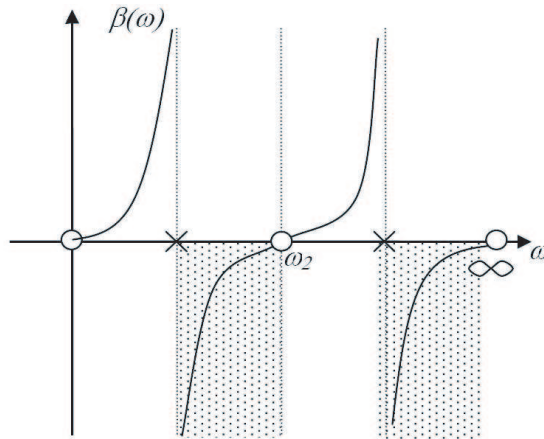
Figure 1. A possible dispersion diagram (real positive function) of a lossless balanced continuous transmission line (shadowed regions: LH bands). In this case the values of K_i constants have been adjusted to obtain zeros at $\omega = 0$, $\omega = \omega_2$ and $\omega = \infty$.

continuous transmission lines can be classified by the order of their distributed immittance functions. From the preceding discussion it follows that the total number of RH and LH regions for a given unit-cell is just the order of its distributed immittance functions.

Equation (6) also provides the circuit model for the distributed series impedance $Z(s)$ and shunt admittance $Y(s)$ of lossless balanced continuous transmission lines of arbitrary order. The partial fraction expansion of the distributed immittance functions defined by (6) (Foster synthesis) yields the generic circuit topology shown in Fig. 2. Other equivalent topologies (Cauer-type networks, for instance) are also valid and could provide alternative design options which could be more appropriate for specific implementations.

3. FIRST LOWER-ORDER LOSSLESS BALANCED TRANSMISSION LINES

The theoretical background presented and discussed in the previous section provides a systematic approach for deriving all possible lossless balanced transmission lines of arbitrary order. The per-unit-length circuit models, and the corresponding frequency responses (dispersion diagrams), of the first eight lower-order transmission lines are depicted in Table 1. In this Table the terms conventional and dual (although not generally accepted) are used to denote those structures with,
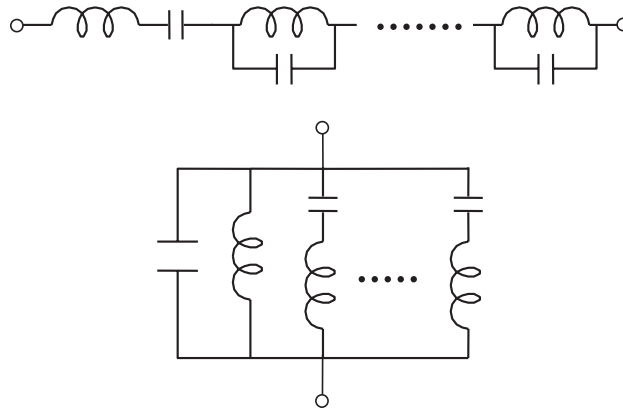
Figure 2. Generic circuit model for the distributed series impedance $Z(s)$ and shunt admittance $Y(s)$ of a lossless balanced continuous transmission line of arbitrary order.

respectively, a zero (RH first frequency band) or a pole (LH first frequency band) at the origin.

It is immediately apparent that the two first-order unit-cells (#1 and #2 in Table 1) correspond to the so-called RH and LH transmission lines, respectively. It is also apparent that the two second-order unit-cells (#3 and #4) are the so-called 'dual' and 'conventional' CRLH transmission lines, respectively, that the double-Lorentz is the first third-order unit-cell (#5), and that the second fourth-order unit-cell (#8) is the so-called 'extended' CRLH transmission line. However, the remaining unit-cells in Table 1 are new. One of them (#6) is a third-order unit-cell (three RH/LH regions) and provides new metamaterial components with potential tri-band performance. The other (#7) is a different fourth-order unit-cell with, obviously, four RH/LH regions and, therefore, potential quad-band applications as its accompanying 'extended' CRLH transmission line.

Obviously, Table 1 can be easily and systematically completed with as many increasing order unit-cells as desired. Nevertheless, it is worth mentioning that no unit-cell with an order greater than four has been proposed so far, thus all of them should also be considered as novel lossless balanced CRLH transmission line unit-cells. The detailed properties and specific applications of these new unit-cells are to be explored.

Table 1. First eight lower-order lossless balanced transmission line per-unit-length circuit models and dispersion diagrams.

	Conventional realization	Schematic dispersion diagram (LH behavior frequency-bands shadowed)
1st #1		
2nd #3		
3rd #5		
4th #7		
	Dual realization	
1st #2		
2nd #4		
3rd #6		
4th #8		

4. ARTIFICIAL LOSSLESS BALANCED TRANSMISSION LINES: STOP-BANDS AND CUTOFF FREQUENCIES

Artificial transmission lines are formed by the cascade interconnection of a sequence of identical (uniform transmission line) symmetrical and reciprocal unit-cells. The resulting periodic network mimics to some extent the propagation characteristics of the ideal continuous transmission line. The aim of this section is to explore the limitations of this periodic network-based implementation. The spatial discretization thusly introduced mainly results in a dispersion diagram with pass-bands and stop-bands (propagation is not possible over an infinite range of frequencies any longer), and therefore in a frequency dependent characteristic impedance which complicates the matching of the structure.

The most appropriate tool for analysing these periodic structures is the image-parameter filter theory. According to this, the properties of a periodic structure can be obtained from the properties of its unit-cell [9]. Therefore only the analysis of the behaviour of the unit-cell is required to infer the behaviour of the whole periodic structure. Since only two parameters, propagation constant and characteristic impedance, are required to fully describe the behaviour of transmission lines (artificial or not), only the image impedance (just one image impedance in the case of symmetric unit-cells) and the propagation factor of the unit-cell have to be calculated. The characteristic impedance of the periodic artificial transmission line is the image impedance of its unit-cell, while the propagation constant is the propagation factor of its unit-cell divided by Δz.

As previously discussed, any lossless balanced continuous CRLH transmission line is fully defined by its normalized distributed (per-unit-length) series impedance $\overline{Z}(\omega)$ or by its normalized distributed (per-unit-length) shunt admittance $\overline{Y}(\omega)$, since $\overline{Z}(\omega) = \overline{Y}(\omega) = j\beta(\omega)$ in the balanced case. The corresponding unit-cell to be cascaded to form the artificial transmission line can be modeled, for instance, by either its T or its Π circuit models (Fig. 3), so there are at least two possible periodic networks, with different performances, for a given continuous transmission line.

The image impedance Z_c and the propagation factor $g = a + jb$ (a and b are the attenuation and phase factors, respectively) of a symmetrical two-port network defined by its transmission ABCD parameters are given by [12]

$$Z_c = \sqrt{\frac{B}{C}}, \tag{7}$$

and

$$g = \cosh^{-1}(A), \tag{8}$$

respectively. The elements of the ABCD matrices of the lossless symmetrical unit-cells of Fig. 3 are

$$A_{\mathrm{T}} = D_{\mathrm{T}} = 1 + \frac{Z_a Y_b}{2}$$
$$B_{\mathrm{T}} = Z_a \left(1 + \frac{Z_a Y_b}{4} \right) \tag{9}$$
$$C_{\mathrm{T}} = Y_b$$

for the T unit-cell, and

$$A_{\Pi} = D_{\Pi} = 1 + \frac{Z_a Y_b}{2}$$
$$B_{\Pi} = Z_a \tag{10}$$
$$C_{\Pi} = Y_b \left(1 + \frac{Z_a Y_b}{4} \right)$$

for the Π unit-cell, with $Z_a = Z_0 \overline{Z}(\omega) \Delta z$, $Y_b = Y_0 \overline{Y}(\omega) \Delta z$, and Δz the 'physical length' of the associated continuous transmission line section. Therefore the image impedances of the unit-cells are

$$Z_{c\mathrm{T}}(\omega) = Z_0 \left[1 - \frac{(\beta(\omega)\Delta z)^2}{4} \right]^{\frac{1}{2}} \tag{11}$$

for the T unit-cell, and

$$Z_{c\Pi}(\omega) = Z_0 \left[1 - \frac{(\beta(\omega)\Delta z)^2}{4} \right]^{-\frac{1}{2}} \tag{12}$$

for the Π unit-cell. These expressions clearly demonstrate that the frequency behaviour of these two image impedances (two possible artificial transmission line implementations) are quite different. However the propagation factor for both implementations is exactly the same and is given by

$$g_{\mathrm{T}}(\omega) = g_{\Pi}(\omega) = a(\omega) + jb(\omega) = \cosh^{-1} \left[1 - \frac{(\beta(\omega)\Delta z)^2}{2} \right] \tag{13}$$

Pass-bands occur at frequencies where the image impedance is purely real, while stop-bands occur at frequencies where the image
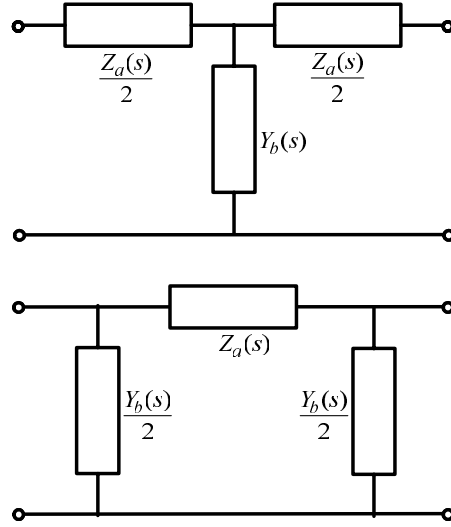
Figure 3. T and Π circuit models of the artificial transmission line unit-cell.

impedance is purely imaginary [10]. Thus transitions between stop-bands and pass-bands occur at frequencies (cutoff frequencies, ω_c) where the expression within the square roots in (11) and (12) vanishes, namely, when

$$|\beta\left(\omega_c\right)| \Delta z = 2 \tag{14}$$

Propagation takes place at frequencies where

$$|\beta(\omega)| \Delta z \leq 2 \tag{15}$$

therefore the main consequence of the spatial discretization of the continuous transmission line is the truncation of the dispersion diagram: no values of $|\beta(\omega)|$ greater than $2/\Delta z$ can be mimicked by the periodic networks defined in Fig. 3. This means that the frequency bands close to the poles of the phase constant of the continuous transmission line can not be emulated by them (Fig. 4 third-order unit-cell #6). That is, in any practical artificial transmission lines based on T or Π circuit models there is always a stop-band around each pole that by no means can be closed up. It is also clear that the bandwidth of these regions are governed by the 'size' (Δz) of the associated continuous transmission line section, that is, by the element values of the cascaded unit-cell: the smaller the value of Δz, the smaller the bandwidth of these stop-bands.
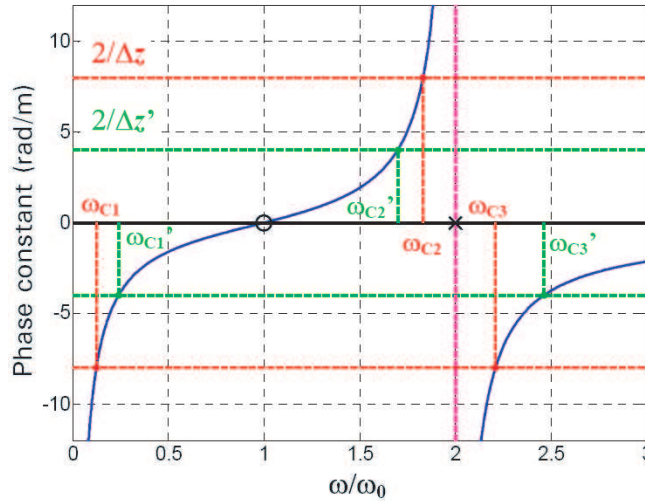
Figure 4. Dispersion diagram (β: blue) of a continuous lossless balanced CRLH transmission line: ω_{Ci}, ω'_{Ci} are the normalized cutoff frequencies introduced by its implementation as a T or Π circuit model-based artificial transmission line for two different values of Δz (artificial-transmission-line section 'size').

Inequality (15) defines the pass-bands of the resulting artificial transmission lines. In such pass-bands the propagation factor is purely imaginary ($g_\text{T}(\omega) = g_\Pi(\omega) = jb(\omega)$) and is given by (13)

$$\cos b(\omega) = 1 - \frac{(\beta(\omega)\Delta z)^2}{2} \tag{16}$$

It should be noted that phase factor value range from $-\pi$ to $+\pi$ within the pass-bands. For small values of $|\beta(\omega)|\Delta z$ Equation (16) yields

$$b(\omega) \approx \beta(\omega)\Delta z \tag{17}$$

This result indicates that any realizable phase constant $\beta(\omega)$ can be mimicked with the desired accuracy by cascading a sufficiently high number of discrete unit-cells with electrical lengths that are much smaller (in magnitude) than π (subwavelength region). However, this condition could be very difficult to fulfill in a particular physical implementation, mainly due to the required values for the elements of the unit-cell, and in fact constitutes the main limitation of artificial CRLH transmission lines.
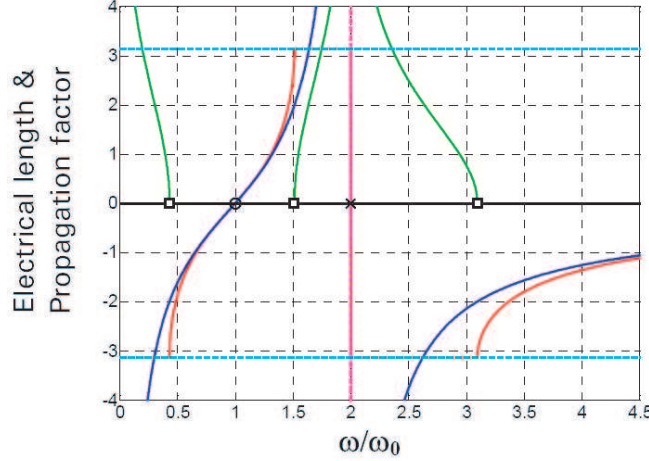
Figure 5. Electrical length of a lossless balanced continuous transmission line and propagation factor of its discrete implementation by a T or Π periodic network for a given value of Δz (third-order unit-cell #6) (ideal continuous electrical length ($\beta \Delta z$): blue; propagation factor ($g = a + jb$), b: red; a: green).

Within the stop-bands the propagation factor is complex. The phase factor can only take one of the two possible values (π or $-\pi$), while the attenuation factor $a(\omega)$ is frequency dependent and is given by

$$a(\omega) = \cosh^{-1}\left[\frac{(\beta(\omega)\Delta z)^2}{2} - 1\right] \tag{18}$$

It is clear that the attenuation factor vanishes at the cutoff frequencies ($a(\omega_c) = 0$) and increases indefinitely as the operation frequency approaches pole frequencies. The relevant differences between the propagation characteristics of the lossless balanced continuous transmission line and its periodic T or Π network-based implementation can be observed in Fig. 5, where a particular case (third-order unit-cell #6) has been depicted for illustrative purposes.

The image impedance for both implementations are given by Equations (11) and (12), and are, as previously commented, purely real within the pass-bands and purely imaginary outside them. It is worth mentioning that the phase constant and the characteristic impedance of both continuous and discrete transmission lines only coincide at the frequency where the phase constant is zero. At any

other frequency both responses are different, and diverge from each other as the operation frequency approaches pole frequencies.

Without going into further detail, the image impedance for the T unit-cell can be expressed, in the stop-bands (defined by $|\beta(\omega)|\Delta z > 2$), as

$$Z_{cT}(\omega) = \pm j Z_0 \left[\frac{(\beta(\omega)\Delta z)^2}{4} - 1 \right]^{\frac{1}{2}} \tag{19}$$

In this expression, the 'plus' and 'minus' solutions correspond to $\beta(\omega) > 0$ and $\beta(\omega) < 0$, respectively, i.e., the image impedance for the T unit-cell is inductive for the frequency range below the pole ($\beta(\omega) > 0$), and capacitive above the pole ($\beta(\omega) < 0$).

Similarly, the image impedance for the Π unit-cell is given, in the stop-bands, by

$$Z_{c\Pi}(\omega) = \mp j Z_0 \left[\frac{(\beta(\omega)\Delta z)^2}{4} - 1 \right]^{-\frac{1}{2}} \tag{20}$$

In this expression, the 'minus' and 'plus' solutions correspond to $\beta(\omega) > 0$ and $\beta(\omega) < 0$, respectively, i.e., the image impedance for the Π unit-cell is capacitive below the pole ($\beta(\omega) > 0$) and inductive above the pole ($\beta(\omega) < 0$). An illustrative example (third-order unit-cell #6) of the frequency behaviour of both image impedances has been depicted in Fig. 6.

Cutoff frequencies are defined by Equation (14). Since the phase constant $\beta(\omega)$ is given by the polynomial defined by Equation (1), the determination of the cutoff frequencies of a given artificial transmission line requires to find the roots of a polynomial with a degree equal to the order of the transmission line. Therefore cutoff frequencies can only be analytically computed for low-order transmission lines (linear, quadratic, cubic or quadratic equations, respectively, for artificial transmission lines up to the fourth-order).

5. A THIRD-ORDER ARTIFICIAL LOSSLESS BALANCED CRLH TRANSMISSION LINE

To illustrate the approach described so far, one of the two third-order artificial lossless balanced CRLH transmission lines is analysed in this section (#6 in Table 1). Let us consider the artificial lossless balanced transmission line defined by the third-order unit-cell shown in Fig. 7.

The dispersion diagram of its associated ideal continuous transmission line is shown in Table 1 (#6). The phase constant has
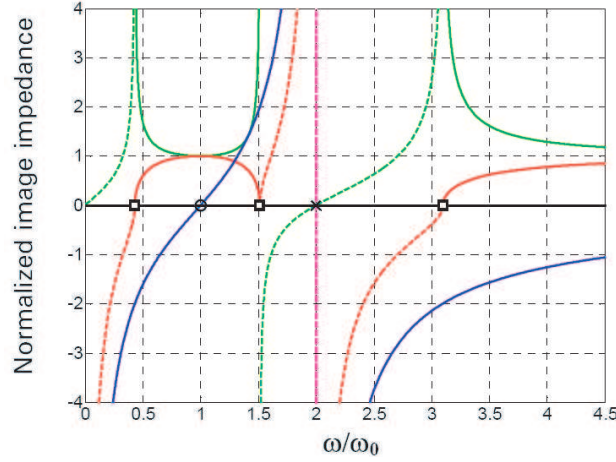
Figure 6. Normalized image impedance as a function of frequency for the discrete implementation of a lossless balanced transmission line (T and Π third-order unit-cell #6) by a periodic network for a given Δz value ($\bar{z}_{c\Pi}$: green, $\bar{z}_{cT}$: red, solid line —— real part; dashed line --- imaginary part). For the sake of clarity the electrical length of the ideal continuous transmission line has been also included ($\beta\Delta z$: blue.

two poles, at $\omega = 0$ and $\omega = \omega_1$, and two zeros, at $\omega = \omega_0$ and $\omega = \infty$. Therefore, it exhibits two LH frequency bands and just one RH frequency band. The location of these frequency bands can be fixed by the designer by just specifying the values for ω_0 and ω_1. The designer can also set the impedance level (Z_0) of the transmission line. It is quite straightforward to show that all the element values defining the unit-cell can be obtained from these parameters (ω_0, ω_1 and Z_0) and C_{0a} or, alternatively, L_{0b}. The required equations are

$$C_{1a} = C_{0a}\frac{\omega_0^2}{\omega_1^2 - \omega_0^2}, \tag{21}$$

$$L_{1a} = \frac{1}{C_{0a}}\frac{\omega_1^2 - \omega_0^2}{\omega_0^2\omega_1^2}, \tag{22}$$

$$L_{1b} = L_{0b}\frac{\omega_0^2}{\omega_1^2 - \omega_0^2}, \tag{23}$$

$$C_{1b} = \frac{1}{L_{0b}}\frac{\omega_1^2 - \omega_0^2}{\omega_0^2\omega_1^2}, \quad \text{and} \tag{24}$$

$$Z_0^2 = \frac{L_{0b}}{C_{0a}} \tag{25}$$
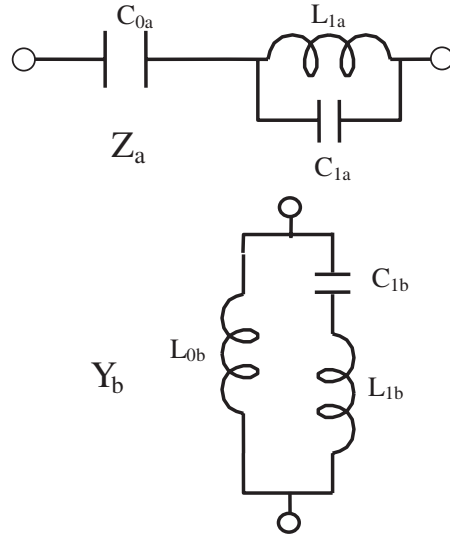
Figure 7. Series impedance (Z_a) and shunt admittance (Y_b) of the third-order artificial lossless balanced CLRH transmission line unit-cell.

The phase constant of the associated ideal continuous transmission line can be expressed as

$$\beta(\omega)\Delta z = \frac{1}{\omega_0\sqrt{L_{0b}C_{0a}}}\frac{\bar{\omega}_1^2\left(\bar{\omega}^2 - 1\right)}{\bar{\omega}^2\left(\bar{\omega}_1^2 - 1\right)} \qquad (26)$$

with $\bar{\omega} = {}^{\omega}\!/_{\omega_0}$, and $\bar{\omega}_1 = {}^{\omega_1}\!/_{\omega_0}$. Fig. 5 depicts the dispersion diagram of this continuous transmission line (Equation (26)) and that of its discrete implementation by the periodic network defined by the unit-cell shown in Fig. 7, Equations (16) and (18), for a particular case: $\omega_0 = 2\pi 10^9 rad/s$, $\omega_1 = 4\pi 10^9 rad/s$, $Z_0 = 50\Omega$, and $C_{0a} = 1pF$. Fig. 5 confirms the expected behaviour of the T or Π periodic network-based implementation: a good emulation of the ideal (continuous) dispersion diagram near the zeros, which degrades as the operation frequency approaches the cutoff frequencies, and the existence of stop-and pass-bands as a result of the discretization. Cutoff frequencies are computed from Equation (14) in conjunction with Equation (26). In this case they can be analytically computed by solving the resulting cubic polynomial.

The different frequency behaviour of the image impedance of T-and Π-based artificial transmission lines is shown in Fig. 6. This
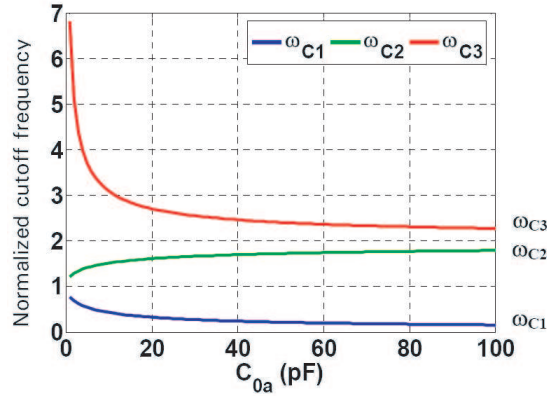
Figure 8. Normalized cutoff frequencies as a function of C_{0a}.
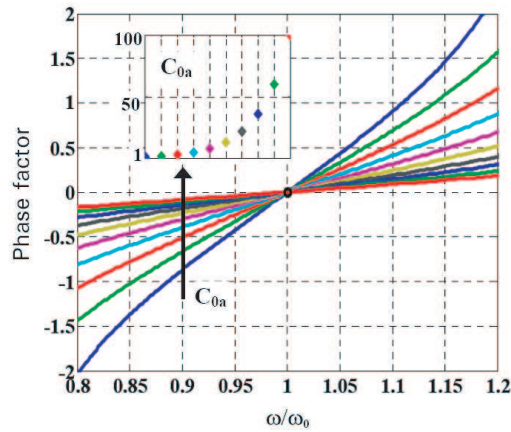
Figure 9. Phase factor ('b' as a function of ω/ω_0) of the artificial transmission line as a function of C_{0a} (in pF; see inset).

figure clearly illustrates the different dispersive behaviours of these two possible implementations.

It is evident that, after fixing the values for ω_0, ω_1, and Z_0, there is only one degree of freedom left: C_{0a} or, alternatively, L_{0b}. This degree of freedom can be used to modify, within certain limits, the location of cutoff frequencies or the slope of the phase factor at $\omega = \omega_0$, for instance. Figs. 8 and 9 depict the influence of C_{0a}, for the particular case under consideration, on these two parameters, and provides, together with the other figures in this section, a rather

complete description of what can be achieved by using this artificial transmission line.

6. CONCLUSIONS AND FURTHER REMARKS

A circuit theory-based investigation of the frequency behaviour of artificial lossless balanced CRLH transmission lines has been presented. The associated ideal continuous transmission line, from which the artificial transmission line is derived, has been used as a simple and efficient model to analyze the limitations of a periodic network-based implementation. It has been shown that artificial lossless balanced transmission lines based on T or Π unit-cells will always exhibit a stop-band around each pole of their associated continuous transmission line that can not be closed up.

This investigation has also yielded the systematic derivation of all possible lossless balanced CRLH transmission lines and the conclusion that the number of RH or LH frequency bands is controlled by the order of its incremental unit-cell. The novel unit-cells obtained in this work as well as those which have already been proposed are just a few examples of lossless balanced artificial transmission lines that can be implemented. As mentioned before, the approach proposed in this work allows the systematic derivation of such transmission line unit-cells of arbitrary order, and thus paves the way for multi-band components based on metamaterial transmission lines.

The physical implementation of artificial lossless balanced CRLH transmission lines deserves some comments. As described, these artificial transmission lines can be formed by the cascade interconnection of a certain number of identical symmetrical and reciprocal lumped-element networks (unit-cells). The required lumped elements can be implemented by using really lumped components such as, for instance, chips in 'surface mount technology' (SMT), or by using 'distributed-lumped' components, where 'distributed-lumped' stands for distributed structures (such as, for instance, transmission line sections) mimicking, up to a certain frequency, the constitutive relation of lumped components [1]. Consequently, the described analysis is only valid up to this frequency, and this happens well before other modes associated to the distributed components can appear. Beyond that frequency the analysis cannot be extrapolated, since the distributed structures no longer mimic the desired lumped element behaviour.

Many novel applications of such low-order artificial transmission lines have been already proposed and designed by using this lumped-element approach (see [1] for an excellent review of this topic). Obviously, the usable frequency range of the resulting artificial

transmission line is limited by the highest frequency at which the components (truly lumped or distributed) can be reasonably considered as lumped. The general properties exhibited by artificial transmission lines, within the frequency band where the lumped description of 'lumped' or 'distributed' components holds, have been dealt with in this paper. In these artificial transmission lines the appearance of stop-bands around the poles is a consequence of the unavoidable discretization required to physically implement them, and they appear at frequencies for which the wavelength in the surrounding environment is large enough (compared to the size of the component) to justify the lumped element description of the constitutive components of the artificial transmission line. In particular, this wavelength has nothing to do with the 'mimicked' wavelength in the artificial transmission line.

Whereas the implementation of higher-order artificial transmission lines may pose some challenges, the present availability of physical realizations for all the required lumped element branches, i.e., series or shunt capacitor and inductor, series or shunt resonant and anti-resonant branches, allows the authors to believe their design and fabrication will not be hampered by any major issue.

Although the discussion is limited to 'balanced' transmission lines, it is evident that 'unbalanced' versions of all the proposed unit-cells can be easily derived by just making the critical frequencies of the distributed series impedance and the distributed shunt admittance different. The main difference between the unbalanced transmission line derived in this manner and any other that could be envisaged is that the former can be 'balanced' whenever required by just 'retuning' its critical frequencies.

ACKNOWLEDGMENT

REFERENCES

1. Caloz, C. and T. Itoh, *Electromagnetic Metamaterials, Transmission Line Theory and Microwave Applications*, Wiley, New York, 2005.

2. Eleftheriades, G. V. and K. G. Balmain (eds.), *Negative-Refraction Metamaterials, Fundamental principles and Applications*, Wiley, New York, 2005.

3. Ramo, S., J. R. Whinnery, and T. van Duzer, *Fields and Waves in Communication Electronics*, Wiley, New York, 1994.

4. Brillouin, L., *Wave Propagation in Periodic Structures*, Dover Publications Inc., New York, 1953.

5. Lai, A., C. Caloz, and T. Itoh, "Composite right/left-handed transmission line metamaterials," *IEEE Microwave Mag.*, Vol. 5, No. 3, 34–50, Sep. 2004.

6. Caloz, C., "Dual composite right/left-handed (D-CRLH) transmission line metamaterial," *IEEE Microw. Wireless Compon. Lett.*, Vol. 16, No. 11, 585–587, Nov. 2006.

7. Rennings, A., S. Otto, J. Mosig, C. Caloz, and I. Wolff, "Extended composite right/left-handed (E-CRLH) metamaterial and its application as quadband quarter-wavelength transmission line," *Asia-Pacific Microwave Conference Digest*, Yokohama, Japan, Dec. 12–15, 2006.

8. Eleftheriades, G. V., "A generalized negative-refractive-index transmission-line (NRI-TL) metamaterial for dual-band and quad-band applications," *IEEE Microw. Wireless Compon. Lett.*, Vol. 17, No. 6, 415–417, June 2007.

9. Rennings, A., T. Liebig, C. Caloz, and I. Wolff, "Double-Lorentz transmission line metamaterials and its applications to tri-band devices," *IEEE MTT-S International Microwave Symposium Digest*, 1427–1430, Honolulu, Hawaii, USA, June 2007.

10. Kuo, F. F., *Network Analysis and Synthesis*, Wiley, New York, 1966.

11. Jachowski, D. R. and C. M. Krowne, "Frequency dependence of left-handed and right-handed periodic transmission structures," *IEEE MTT-S International Microwave Symposium Digest*, 1831–1834, Fort Worth, Texas, USA, June 6–11, 2004.

12. Elliot, R. S., *An Introduction to Guided Waves and Microwave Circuits*, Prentice Hall, Englewood Cliffs, 1993.